

# Transparent and conductive ZnO:Al thin films prepared by sol-gel dip-coating

G.G. Valle, P. Hammer, S.H. Pulcinelli, C.V. Santilli\*

*Instituto de Química, UNESP, PO Box 355, 14800-970, Araraquara, S.P., Brazil*

## Abstract

Aluminum doped zinc oxide polycrystalline thin films (AZO) were prepared by sol-gel dip-coating process. The sol was prepared from an ethanolic solution of zinc acetate using lithium hydroxide or succinic acid as hydrolytic catalyst. The quantity of aluminum in the sol was varied from 1 to 10 mol%. The structural characteristics studied by X-ray diffractometry were complemented by resistivity measurements and UV–Vis–NIR spectroscopy. The films are transparent from the near ultraviolet to the near infrared, presenting an absorption cut-off at almost 290 nm, irrespective of the nature of the catalyst and doping level. The best conductors were obtained for the AZO films containing 3 mol% of aluminum, prepared under acidic and basic catalysis and sintered at 450 °C. Their optical band-gap of 4.4 eV calculated from the absorption cut-off is larger than the values for band-gap widening predicted by the standard model for polar semiconductors. These polycrystalline films are textured with preferential orientation of grains along the wurtzite *c*-axis or the (100) direction.

© 2003 Elsevier Ltd. All rights reserved.

**Keywords:** Aluminum doping; Conductivity; Sol-gel; Zinc oxide films

## 1. Introduction

Zinc oxide films exhibit a combination of interesting piezoelectric, electrical, optical and thermal properties, which are already applied in the fabrication of a number of devices, such as gas sensors,<sup>1</sup> ultrasonic oscillators<sup>2</sup> and transparent electrodes in solar cells.<sup>3</sup> Several techniques were employed to produce pure and doped ZnO films, including chemical vapor deposition,<sup>1</sup> sputtering,<sup>2</sup> spray pyrolysis,<sup>3–5</sup> and the sol-gel process.<sup>6,7</sup> Among the preparation techniques of ZnO films, the sol-gel route proposed by Spanhel and Anderson,<sup>8</sup> in combination with the dip-coating process, represents an easy low cost and efficient route to coat large surfaces, permitting also the tailoring of the microstructure from the chemistry of the sol-gel synthesis. On the other hand, nanocrystalline ZnO films produced by these techniques suffer quality limitation, in respect to their electrical and optical properties, due to the high density of carrier traps and potential barriers at grain boundaries. However, in several studies it was shown that the opto-electrical properties could be considerably improved by optimized deposition

conditions and doping.<sup>4,5</sup> The indium doped ZnO films grown at deposition temperatures of 400 and 450 °C showed an improved crystallinity (texturization along the *c*-axis) leading to a strong decrease of the resistivity. Besides indium, also aluminum is a promising dopant to improve the opto-electrical properties of ZnO films.<sup>8</sup>

In the present work we have investigated the influence of preparation conditions on the structural, electrical and optical properties of aluminum doped ZnO films. The films were prepared from colloidal suspensions containing different Al concentrations and deposited by dip-coating on glass substrates. The structural characteristics were studied by X-ray diffractometry and the electrical and optical properties were investigated by resistivity measurements and UV–Vis spectroscopy, respectively.

## 2. Experimental

A 0.1 mol  $L^{-1}$  zinc organometallic precursor solution  $Zn_4O(COOCH_3)_6$  was synthesized from zinc acetate dihydrate  $[Zn(Ac)_2 \cdot 2H_2O]$  dissolved in absolute ethanol and heated under reflux for 3 h at 80 °C. Then the precursor solution was hydrolyzed in acidic ( $[H^+]/[Zn^{2+}] = 0.1$ ) or basic ( $[OH^-]/[Zn^{2+}] = 0.1$ ) environment

\* Corresponding author. Tel.: +55-16-2016645; fax: +55-16-222-7932.

E-mail address: [santilli@iq.unesp.br](mailto:santilli@iq.unesp.br) (C.V. Santilli).



with a solution containing succinic acid or lithium hydroxide, respectively. The molar ratios of dopant (aluminum isopropoxide) in the solution, [Al/Zn], was varied between 1 and 10%.

AZO films were deposited on cleaned Corning boron-silicate glass substrates by the dip-coating method. Every deposition involved 10 dips at a lifting speed of 8 cm/min. After the deposition, the samples were dried at 100 °C and fired at 450 °C. The total thickness of the films was in the range of 200 to 300 nm.

The crystalline structure was analyzed by X-ray diffraction (XRD) using a Siemens D5000 diffractometer (Cu  $K_\alpha$ ) and the electric resistivity was measured using evaporated gold electrodes at the surface of the films. The optical properties were studied by UV–Vis–NIR spectrometry (500 Scan, Varian). The spectra were taken using the Corning glass reference with a cut-off wavelength at 280 nm.

### 3. Results and discussion

All AZO films are nanocrystalline and exhibit the wurtzite structure with all XRD peaks identified in the recorded range. The XRD patterns measured for AZO films deposited from precursor solutions prepared by acidic (succinic acid) and basic hydrolysis (lithium hydroxide) are compared in Fig. 1a and b, respectively. From the evolution of the diffraction patterns with the doping concentration in the precursor solution it can be observed that the quantity of Al doping determines the orientation of the nanocrystals. The film prepared by acidic catalysis (Fig. 1a) using a molar ratio Al/Zn of 3% shows a preferential orientation of grains along the  $c$ -axis, perpendicular to the film surface (002). At higher Al concentrations the preferential orientation changes to (100) with a small contribution of (002) and (101) directions at highest Al content. Films prepared by basic catalysis (Fig. 1b) show up to a Al concentration of 3% a preferential crystal grow along the (100) direction. For higher Al content the presence of the three principal peaks of the wurzite lattice, i.e. (100), (002) and (101), reveal a random orientation of the nanocrystals.

Quantitative information concerning the preferential crystallite orientation was obtained from the texture coefficient,  $T_C$ , defined as:<sup>9</sup>

$$T_C(hkl) = \frac{I(hkl)}{I_r(hkl)} / \frac{1}{n} \sum \frac{I(hkl)}{I_r(hkl)} \quad (1)$$

where  $n$  is the number of the diffraction peaks,  $I(hkl)$  and  $I_r(hkl)$  denote the integrated intensities corresponding to (hkl) reflections of samples containing textured and randomly oriented grains, respectively. The value  $T_C(hkl)=1$  represents films with randomly oriented crystallites, while higher values indicate the abundance of grains oriented in a given (hkl) direction. The varia-

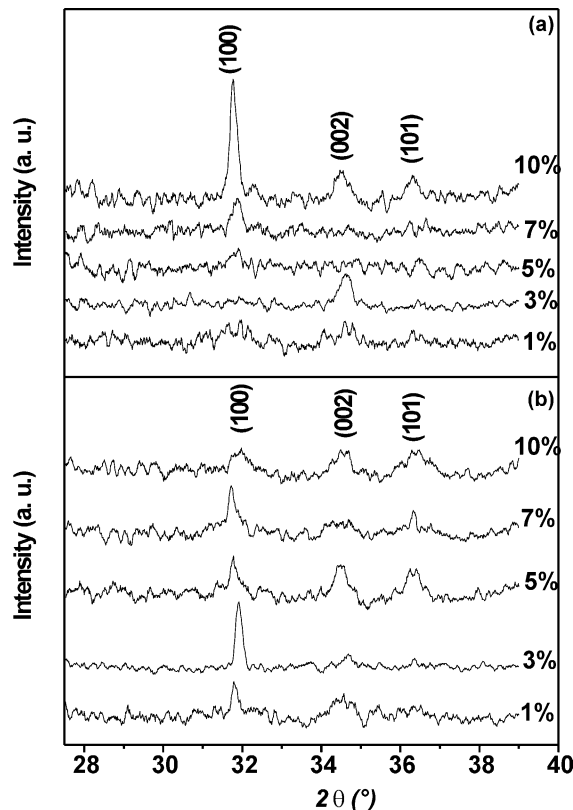


Fig. 1. Evolution of the X-ray diffraction patterns of films prepared, at different molar ratios Al/Zn in the precursor solution, by acidic (a) and basic (b) catalysis.

tion of  $T_C$  for the three main peaks of the wurzite lattice, are presented in Table 1. Included are also the values of the average crystallite size,  $D$ , determined by Sherrer's formula.

For films prepared by acidic catalysis the calculated  $T_C$  values increase along the (100) direction and decrease along the (002) direction with rising Al concentration. This behavior is accompanied by the increase of average crystallite size in the (100) plane from 20 to 47 nm. The doping effect on the texturization is less pronounced for samples prepared by basic catalysis. Only the film prepared at Al/Zn = 3%, containing grains of about 20 nm, shows a texturization along the (100) direction.

All ZnO films containing different Al doping concentrations were highly transparent from the near ultraviolet to the near infrared with a transmittance of more than 80% (not shown). The cut-off wavelength at about 290 nm corresponds to a value of 4.3 eV, which is considerably larger than the optical band-gap of monocrystalline ZnO (3.5 eV). The absorbance spectra of samples deposited from acidic and basic solutions are compared in Fig. 2. Independent on the nature of the catalyst an increasing absorption with raising Al content can be observed in the near UV region. Furthermore, a large shoulder in the range between 330 and 370



Table 1

Texture coefficient,  $T_C$ , the average crystallite size,  $D$ , and density,  $\rho$ , for different crystallographic orientations of ZnO:Al films for different molar ratios, Al/Zn, in the precursor solution prepared by acidic and basic catalysis

Al/Zn [%]	Acidic catalysis							Basic catalysis						
	$T_C$			$D$ [nm]			$\rho$ [g/cm <sup>3</sup> ]	$T_C$			$D$ [nm]			$\rho$ [g/cm <sup>3</sup> ]
	(100)	(002)	(101)	(100)	(002)	(101)		(100)	(002)	(101)	(100)	(002)	(101)	
1	1.1	1.7	1.8	22	47	18	2.9	5.9	1.5	—	69	17	—	2.8
3	— <sup>a</sup>	2.1	0.4	—	24	—	3.7	3.1	—	—	20	—	—	3.9
5	3.8	—	0.1	20	—	—	3.3	5.4	1.5	1.0	57	25	20	3.2
7	3.7	—	0.1	39	—	—	3.2	4.2	1.2	0.7	58	20	12	3.1
10	4.3	1.2	1.3	47	22	26	3.3	1.4	1.6	1.1	19	17	11	3.2

<sup>a</sup> No peak identification possible.

nm is visible in the absorbance spectra. This excitonic peak is related to the quantum confinement effect due to nanoscopic size of the crystallites. The position of this peak depends on the grain size by the relation:<sup>10</sup>

$$\frac{1240}{\lambda_{1/2}} = a + \frac{b}{D^2} - \frac{c}{D} \quad (2)$$

where  $\lambda_{1/2}$  corresponds to the wavelength at 50% of the peak intensity and the constants  $a=3.301$ ,  $b=294$ ,  $c=-1.09$ . These empiric values allow for a adequate description of the relation between  $\lambda_{1/2}$  and crystallite size,  $D$ , between 6.5 and 39 nm.

For samples prepared by acidic catalysis (Fig. 2a), the position of  $\lambda_{1/2}$  is varying, depending on the Al concentration, between 365 and 374 nm with corresponding grain sizes between 6.8 and 18 nm. For samples prepared by basic catalysis (Fig. 2b) and  $\lambda_{1/2}$  between 367 and 370 nm the crystallite size was found between 6.8 and 8.8 nm. These values are somewhat smaller than those calculated from the diffraction peaks.

The optical band-gap,  $E_g$ , was determined from the absorption spectra using equation:<sup>11</sup>

$$(\alpha h\nu)^2 = C(h\nu - E_g) \quad (3)$$

related to direct transitions in ZnO crystals, with constant  $C$  depending on the electron-hole mobility.

The  $(\alpha h\nu)^2$  vs.  $h\nu$  plots are displayed in Fig. 3. Independent on the preparation method (acidic or basic catalysis) the determined optical band-gap of the samples is varying, depending on the Al concentration, between 4.15 and 4.43 eV. The largest values of  $E_g$  was determined for the textured films ((002) or (100) orientation) prepared from solutions containing 3% Al (Fig. 3a,b). The value of 4.43 eV is notably larger than the optical band-gap reported for similar films<sup>8</sup> or even for monocrystalline ZnO. In general the blue shift of the absorption onset of Al doped nanocrystalline films is associated with the increase of the carrier concentration blocking the lowest states in the conduction band, well known as the Burstein–Moss effect.<sup>12</sup> The theory for band-gap widening for polar semiconductors, proposed by Sernelius et al.,<sup>8</sup> in order to describe the experimentally found blue shift in Al doped ZnO films, considers displacement polarization effects and structural disorder as additional factors that affect the shape of the band tails. Although the band-gap widening of the most of the studied films can be justified by this model, the band-gap values of more than 4.4 eV, found in textured samples containing relatively small crystallites ( $\sim 20$  nm), are not well understood. It is suggested that also quantum confinement phenomena induced by the nanoscopic size of the crystallites contribute to this effect.

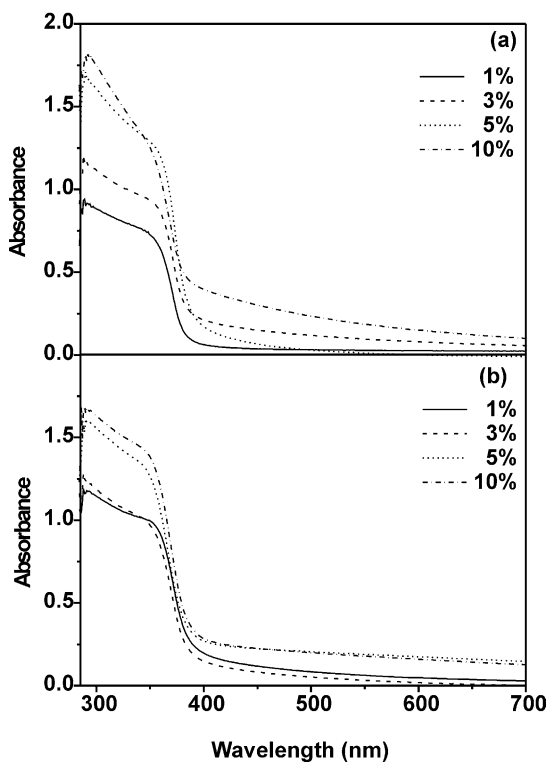


Fig. 2. Evolution of the absorbance spectra of films prepared, at different molar ratios Al/Zn in the precursor solution, by acidic (a) and basic (b) catalysis.



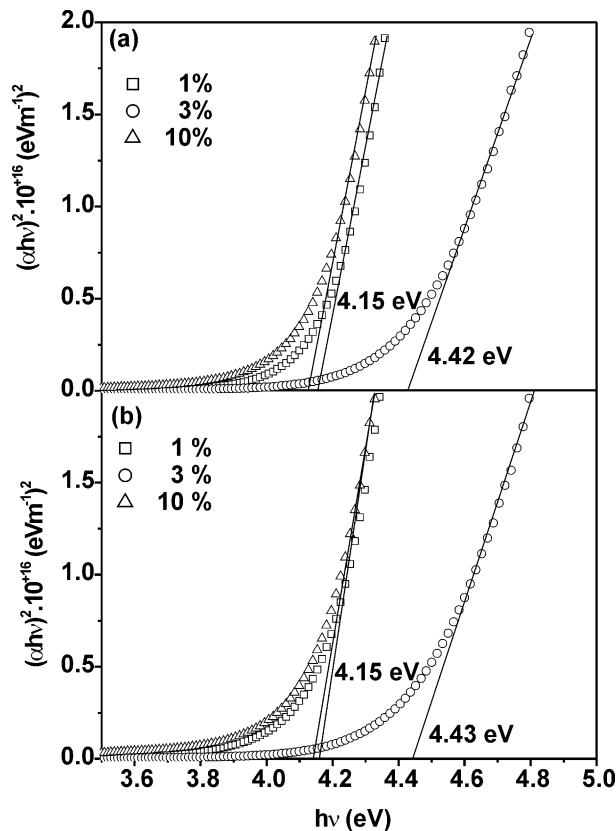


Fig. 3. Evolution of the  $(\alpha h\nu)^2$  vs  $h\nu$  curves of films prepared, at different molar ratios Al/Zn in the precursor solution, by acidic (a) and basic (b) catalysis.

The influence of increasing quantity of aluminum doping on the electrical properties of ZnO films was studied from DC current ( $I$ )-voltage ( $V$ ) characteristics. Irrespective of the type of the catalysis and Al concentration all studied films present a linear  $I$  vs  $V$  dependence, typical of Ohmic behavior. However, the resistivity values of the films, ranging between  $4.1 \times 10^4$  and  $2.7 \times 10^7 \Omega \text{cm}$ , are considerably higher than those reported for comparable samples in the literature.<sup>4,5,8</sup> The results of mass density measurements (Table 1), performed by X-ray reflectometry, indicate that one reason for the high resistivity of the studied films might be their porous structure. Compared with the mass density of  $5.6 \text{ g/cm}^3$  for monocrystalline ZnO, the obtained values in the range of 2.8 to  $3.9 \text{ g/cm}^3$  correspond to porosity between 50 and 30%. As expected, the lowest resistivity exhibits the less porous films, prepared from precursor solutions containing 3% of Al-doping. There is a clear relationship between the improvement of the opto-electrical properties and the nanostructure formed at intermediate Al content. The addition of 3% Al favors efficient electronic doping (substitutional incorporation of Al) and possibly increase of the number of nucleation centers leading to the formation of small preferentially oriented grains, thus inducing a densification of the material. These effects results in a significant decrease of resistiv-

ity and increase of the optical band-gap. The absence of texturization, grains with varying size and the high porosity characterize the structure of films prepared at Al/Zn ratios other than 3%. Consequently, the high resistivity of these films can be attributed both, to the reduced grain boundary area, which leads to few continuous electrical conductive ways, and to the boundary carrier scattering due to the presence of adsorbed gas species and segregation of Al for samples containing high Al/Zn ratios ( $> 3\%$ ).

#### 4. Conclusions

The results of the structural analysis of Al doped ZnO films prepared by the sol-gel dip-coating process evidence that the nanostructure of films containing an intermediate Al concentration (Al/Zn = 3%) is clearly different than those prepared with lower or higher quantity of the dopant.

For the former films, the texturization along the (002) c-axis (basis catalysis) and (100) direction (acidic catalysis) has a significant influence on their electrical and optical properties. The resistivity of these more compact films is three orders of magnitude lower than for those with other Al content. The optical band-gap of about 4.4 eV is considerably larger than that of monocrystalline ZnO and cannot be described by the standard theories for band-gap widening.

The nanostructure of films with other Al content consists of randomly orientated nanocrystals with grain size increasing with the Al concentration. The high electric resistivity of Al-doped ZnO films can be explained by the high porosity of the material and the high number of potential barriers and traps for conducting electrons at the grain boundaries.

#### Acknowledgements

This work has been supported by CAPES and FAPESP (Brazil).

#### References

1. Nishino, J., Kawarada, T., Ohisho, S., Saitoh, H., Maruyama, K. and Kamata, K., Conductive indium-doped zinc oxide films prepared by atmospheric-pressure chemical vapour deposition. *J. Mater. Sci. Lett.*, 1997, **16**, 629–631.
2. Wang, R., King, L. L. H. and Sleight, A. W., Highly conducting transparent thin films based on zinc oxide. *J. Mater. Res.*, 1996, **11**, 1659–1664.
3. Messaoudi, C., Sayah, D. and Abd-Lefdil, M., Transparent conducting undoped and indium-doped zinc-oxide films prepared by spray-pyrolysis. *Phys. Stat. Sol.*, 1995, **151**, 93–97.
4. Tokumoto, M. S., Smith, A., Santilli, C. V., Pulcinelli, S. H., Elkaim, E. and Briois, V., Effect of In concentration in the start-



- ing solution on the structural and electrical properties of ZnO films prepared by the pyrosol process at 450 °C. *J. Non-Cryst. Solids*, 2000, **273**, 302–306.
5. Tokumoto, M. S., Smith, A., Santilli, C. V., Pulcinelli, S. H., Craievich, A. F., Elkaim, E., Traverse, A. and Briois, V., Structural electrical and optical properties of undoped and indium doped ZnO films prepared by the pyrosol process at different temperatures. *Thin Solid Films*, 2002, **416**, 284–293.
  6. Schuler, T. and Aegerter, M. A., Optical, electrical and structural properties of sol gel ZnO:Al coatings. *Thin Solid Film*, 1999, **351**, 125–131.
  7. Tokumoto, M. S., Pulcinelli, S. H., Santilli, C. V. and Craievich, A. F., SAXS study of the kinetics of formation of ZnO colloidal suspensions. *J. Non-Cryst. Solids*, 1999, **247**, 176–182.
  8. Sernelius, B. E., Berggren, K. F., Jin, Z., Hamberg, I. and Granqvist, C. G., Band-gap tailoring of ZnO by means of heavy Al doping. *CPhys. Rev. B*, 1998, **37**, 10244–10248.
  9. Garret, C. S. and Massalski, T. B., *Structure of Metals*. Pergamon Press, Oxford, 1980.
  10. Meulenkaamp, E., A., Synthesis and growth of ZnO nanoparticles. *J. Phys. Chem. B*, 1998, **102**, 5566–5572.
  11. Tauc, J., Grigorovich, R. and Vancu, A., Optical properties and electronic structure of amorphous germanium. *Phys. Status Solidi.*, 1966, **15**, 627–633.
  12. Burstein, E., Anomalous optical absorption limit in InSb. *Phys. Rev.*, 1954, **93**, 632–633; Moss, T. S., The Interpretation of the properties of indium antimonid. *Proc. Phys. Soc. London, Ser. B*, 1954, **67**, 775–782.